Available online at www.sciencedirect.com
ScienceDirect
Journal of Nuclear Materials 363–365 (2007) 539–543
journal of nuclear materials
www.elsevier.com/locate/jnucmat

Numerical analysis of the SOL/divertor plasma flow with the effect of drifts

K. Hoshino [a], A. Hatayama [a,*], N. Asakura [b], H. Kawashima [b], R. Schneider [c], D. Coster [d]

[a] *Faculty of Science and Technology, Keio University, Yokohama 223-8522, Japan*
[b] *Naka Fusion Institute, Japan Atomic Energy Agency, 311-0193, Japan*
[c] *Max-Planck-Institut für Plasmaphysik, Greifswald, Germany*
[d] *Max-Planck-Institut für Plasmaphysik, Garching, Germany*

Abstract

The effects of drifts on parallel plasma flows have been studied. Numerical calculations using a 2D edge plasma simulation code (the SOLPS 5.0 code) have been done for the analysis of JT-60U W-shaped divertor plasmas in the detached state. Although significant effects of drifts on parallel plasma flows have not been observed in the inner and outer divertor regions, the flow reversal due to drifts has been observed at the outer mid-plane. The Pfirsch–Schlüter flow possibly explains the flow reversal.

PACS: 52.25.Fi; 52.30.−q; 52.55.Fa; 52.65.−y

Keywords: Drift effects; SOL plasma flow; Divertor detachment; B2.5-Eirene; JT-60U

1. Introduction

In order to clarify divertor plasma characteristics, such as in–out asymmetry, impurity transport and detachment characteristics, understanding of SOL/divertor plasma flows and their spatial structure is very important. In the divertor region, high parallel flows associated with plasma detachment have been observed in several tokamak experiments [1,2]. Large Mach flows up to Mach 1 or even larger have been measured near the X-point away from the target plate in these experiments. (Henceforth, abbreviation 'HMAD' will be used for such high Mach flows associated with the detachment.) Recently, numerical simulation using B2-Eirene SOLPS 4.0 code [3–5] has been done to clarify the physical mechanism of the HMAD [6,7]. In addition, effects of $\mathbf{E}\times\mathbf{B}$ and diamagnetic drifts on the HMAD have been studied by using B2.5-Eirene SOLPS 5.0 code [8–10] in Refs. [11,12]. These studies mainly focused the attention on the plasma flow only in the divertor region under the detached state.

* Corresponding author. Address: 3-14-1 Hiyoshi, Kouhoku-ku, Yokohama-shi 223-8522, Japan. Tel.: +81 45 566 1607; fax: +81 45 566 1587.
E-mail addresses: khoshino@ppl.appi.keio.ac.jp (K. Hoshino), akh@ppl.appi.keio.ac.jp (A. Hatayama).

0022-3115/$ - see front matter © 2006 Elsevier B.V. All rights reserved.
doi:10.1016/j.jnucmat.2006.12.031

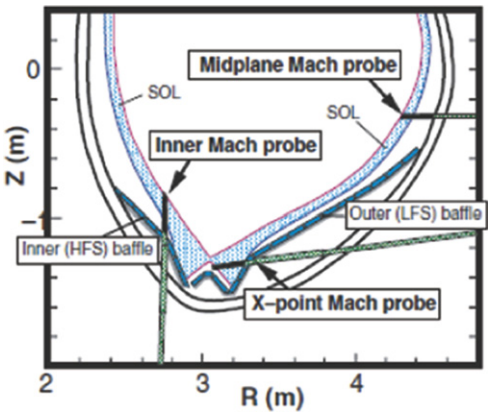

Fig. 1. The locations of the reciprocating Mach probes used in the JT-60U experiment (cited from Ref. [13]).

Recently, in JT-60U, a reciprocating Mach probe was installed above the inner baffle in addition to the outer mid-plane and just below the X-point as shown in Fig. 1 [13]. The flow reversal, i.e., plasma flow from divertor region toward the top of plasmas, is observed at outer mid-plane in the attached state. The driving mechanism of flow reversal was studied in Refs. [2,13,14]. One of the candidate mechanisms of flow reversal was effects of drifts. The effect of drifts on parallel flow was verified by the UEDGE simulation with a simple neutral fluid model under the attached state [13,14].

In this paper, effects of drifts not only on the HMAD, but also overall SOL/divertor parallel plasma flow in the detached phase are analyzed by a numerical simulation. Neutral behavior has been simulated by kinetic neutral transport code (Eirene code [4,15]) instead of a simple neutral fluid model, since the neutral transport has an important role especially in the detached plasma.

2. Numerical model

The B2.5-Eirene SOLPS 5.0 code package [8–10] has been applied to an analysis of JT-60U W-shaped divertor plasmas. Bulk ion species D^+ and all carbon impurity ion species, C^+–C^{6+}, are considered, and are described in the fluid approximation by the B2.5 multi fluid code [8–10]. The particle balance, the parallel momentum balance, the ion and electron energy balance, and the current continuity equations are solved simultaneously. The detailed description of these basic equations and the expression for the perpendicular (radial) and poloidal velocity components including drifts and diffusive terms have been already given in Ref. [10]. In the present analysis, we focused on the plasma flow in the SOL and divertor region. Drifts in the core region are effectively switched off even in the case with drifts. More specifically, drift terms in the core region are multiplied by a function $F(r) = 0.5(1 + \tanh(r + 0.1)/0.015)$, where r is a distance from separatrix in the core region ($r < 0$). In Ref. [10], the potential profile in the SOL region has not been significantly changed between the cases with and without drifts because the potential on the open field lines is mainly determined by the parallel momentum balance equation for electrons. The anomalous transport coefficients for the perpendicular particle and energy transport are taken to be $D = 0.3\ \mathrm{m^2/s}$ and $\chi_i = \chi_e = 2.0\ \mathrm{m^2/s}$, respectively. On the other hand, the parallel transport along field lines in the SOL region is assumed to be classical.

These plasma descriptions by the B2.5 fluid code are self-consistently coupled to the Eirene Monte Carlo code [4,15] for the neutrals. Essential features of neutral dynamics for D, D_2 and C are taken into account by the Eirene code.

Fig. 2 shows the numerical mesh generated from the JT-60U MHD equilibrium of a shot #029623. This shot is a typical of the large volume, L mode discharges for JT-60U. The basic plasma parameters of this shot are as follows: the plasma current $I_p = 1.2$ MA, the toroidal magnetic field $B_t = 3.5$ T and the effective safety factor $q_{eff} = 4.4$.

The boundary conditions are as follows: at core interface boundary, bulk ion density is fixed to $n_D^{Core} = 2.8 \times 10^{19}\ \mathrm{m^{-3}}$ for the detached state and total energy input of 2.5 MW equally is split between the ion and electron channels are assumed. As boundary condition at wall side, radial decay length of 1 cm for the densities and temperatures of the ions and electrons is used. The remaining boundary conditions at plates, walls and core interface boundary are the same as those in Refs. [11,12].

3. Numerical results

Fig. 3 shows the parallel Mach number along the poloidal field line from the inner divertor to the outer divertor at 8 mm outside from the separatrix on the outer mid-plane. The cases with and without drifts are shown by the solid and broken lines, respectively. The poloidal distance $L = 0$ m and $L = 7.38$ m are the inner and outer divertor targets, respectively. The Mach number away from the target plate increases up to about $|M| \sim 1$ at

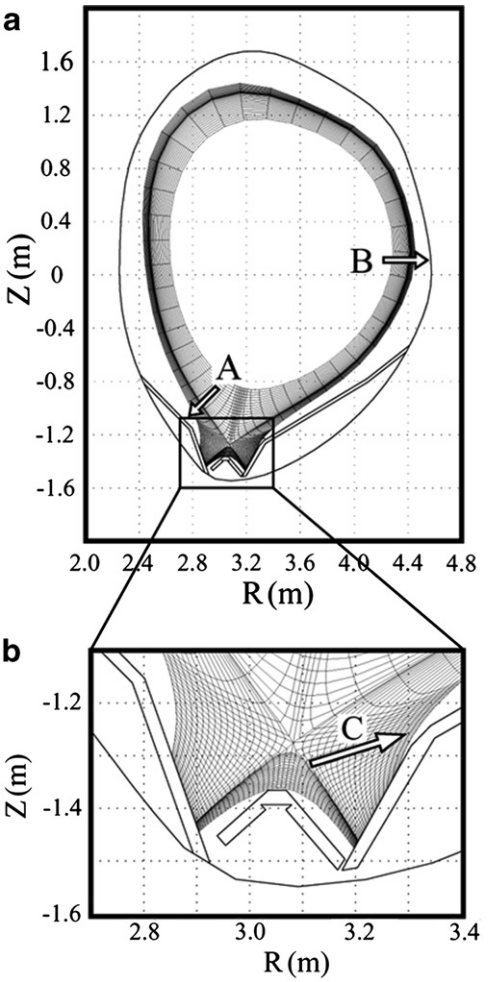

Fig. 2. The JT-60U geometrical configuration: (a) numerical grids for the analysis and the vacuum vessel and (b) zoom-in view of the divertor region. The radial profiles of parallel flow velocity will be discussed along the arrows A, B and C later in Fig. 4. These arrows are chosen to be almost the same path as those of the reciprocating Mach probes used in JT-60U experiments [13] shown in Fig. 1.

$L \sim 0.08$ m and $|M| \sim 0.8$ at $L \sim 7.34$ m. The HMAD appears in the both of the inner and the outer divertor regions. As was discussed in Refs. [6,7,11,12], the HMAD is driven mainly by the pressure gradient force in the parallel direction away from the targets due to the detachment. In Fig. 3, positive and negative signs correspond to the flow toward the outer divertor and the inner divertor, respectively. A negative Mach number ($M < 0$) region, i.e., flow reversal appears around the outer mid-plane ($L \sim 5.78$ m). The flow velocity toward the plasma top increases due to the effect of drifts, especially in the region 3.23 m $< L <$ 7.05 m.

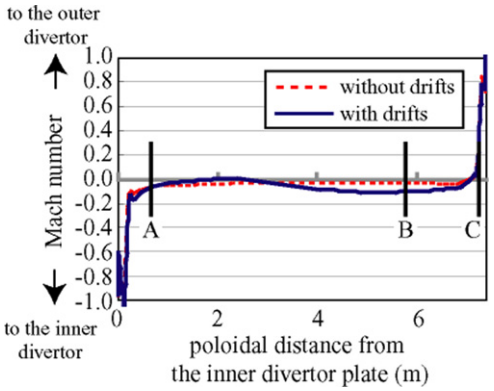

Fig. 3. The Mach number is plotted along the poloidal field line from the inner divertor to the outer divertor near the separatrix. The locations of the arrows A, B and C in Fig. 2 correspond to the poloidal positions at $L = 0.66$ m, $L = 5.78$ m and $L = 7.24$ m, respectively.

In Fig. 4, parallel Mach numbers are plotted along the path shown by the arrows A, B and C in Fig. 2. The profiles are mapped onto the outer mid-plane. The circle and square symbols show the cases without and with drifts, respectively. In Fig. 4(a), the Mach number is negative in all the SOL region. The direction of plasma flow is toward the inner target. In Fig. 4(c), the Mach number has a peak $M \sim 0.7$ near the separatrix, and the HMAD can be seen. The significant effects of drifts on plasma flows in the divertor region cannot be seen in Fig. 4(a) and (c), mainly because of the smaller pressure gradient, the low electron temperature and the resultant small radial electric field due to the detachment as was discussed in Refs. [11,12].

At the outer mid-plane (Fig. 4(b)), flow reversal is observed especially in the case with the drifts. The similar tendency, i.e., flow reversal at the outer mid-plane has been reported by the experiment and the UEDGE code simulation [13,14] though they are under the attached state. On the other hand, in the case without drifts, the radial width of flow reversal region is narrow and the magnitude of the Mach number is small.

The radial profiles of the poloidal $\mathbf{E} \times \mathbf{B}$ drift velocity v_E and the poloidal diamagnetic drift velocity v_D at the outer mid-plane are shown in Fig. 5. The triangle, square and circle symbols show $\mathbf{E} \times \mathbf{B}$ drift, diamagnetic drift and the sum of them, respectively. The magnitude of v_D is relatively large due to the relatively large pressure gradient at the mid-plane. The direction of diamagnetic drift is toward the outer divertor region. On the other hand, $\mathbf{E} \times \mathbf{B}$ drift directs mainly toward the plasma

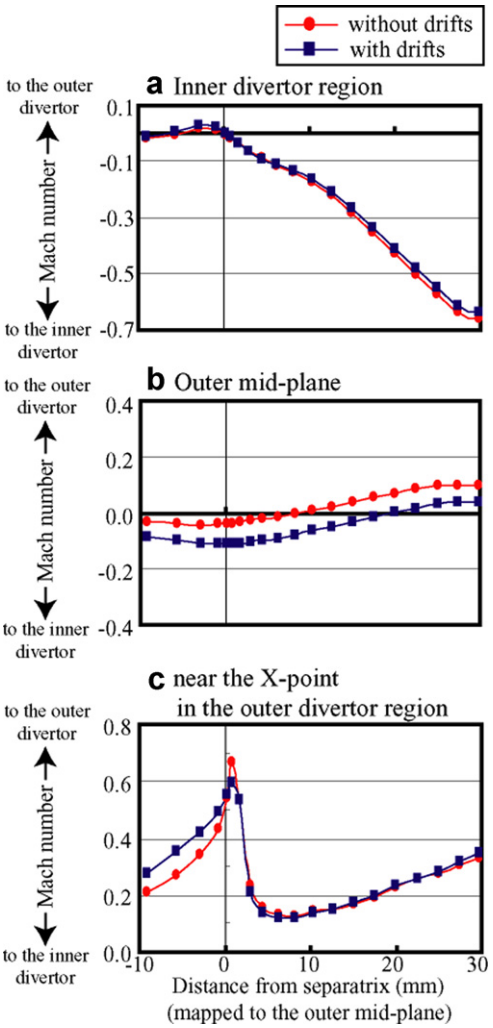

Fig. 4. The radial profiles of the parallel Mach number are plotted along the path shown by the arrows in Fig. 2: (a) at the inner divertor region, (b) at the outer mid-plane and (c) near the X-point. The profiles are mapped onto the outer mid-plane.

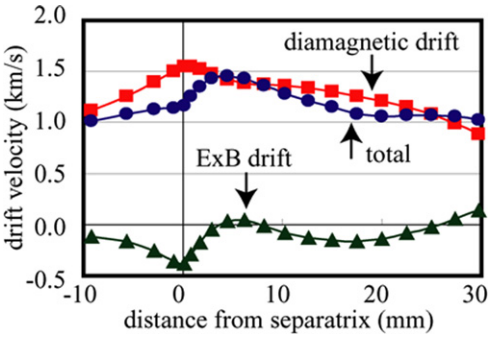

Fig. 5. The radial profile of the poloidal drift velocity at the outer mid-plane. The triangle, square and circle symbols show $\mathbf{E}\times\mathbf{B}$ drift, diamagnetic drift and the sum of them, respectively.

top. However, $|v_E|$ is smaller than $|v_D|$, because both the electron temperature and its gradient are small. As a result, the net particle flux by the poloidal drifts is relatively large, and directs toward the outer divertor region. The particle flux by drifts does not affect directly parallel plasma flows because drifts are perpendicular to a field line. However, in order to satisfy the current continuity equation $\nabla\cdot\mathbf{J}=0$, the parallel ion flux is driven by drifts, i.e., the Pfirsch–Schlüter flow is driven as pointed out in Ref. [2].

The Pfirsch–Schlüter flow velocity at the outer mid-plane can be estimated by a simple expression [16], $v_{PS}=-2(r/R)(1/B_p)\ (\mathbf{E}_r-\nabla_r p/en)$, where B_p, r, R, $\mathbf{E}_r$, p, e and n are the poloidal magnetic field, the minor radius, the major radius, the radial electric field, the pressure, the electric charge and the ion density, respectively. From the simulation result, the above expression gives $|v_{PS}|\sim 5.5$ km/s near the separatrix, and the direction is toward the plasma top. In the simulation result without drift effects, parallel flow velocity near the separatrix is $|v_{\text{no drift}}|\sim 2.5$ km/s. The sum of these velocities becomes $|v_{\parallel}^{\text{estimate}}|=|v_{PS}+v_{\text{no drift}}|\sim 8$ km/s. The value of $|v_{\parallel}^{\text{estimate}}|$ is almost equal to the parallel flow velocity with drift effects $|v_{\parallel}|\sim 8.3$ km/s in the simulation. Thus the driving mechanism of the flow reversal is mainly explained by the Pfirsch–Schlüter flow, especially by effects of diamagnetic drift under the present simulation conditions.

4. Summary and future study

To investigate effects of drifts on parallel plasma flows in the SOL and divertor region, the B2.5-Eirene SOLPS 5.0 simulation of JT-60U W-shaped divertor plasmas has been done. In the present analysis, we mainly focused our attention on the detached state.

At the outer mid-plane, flow reversal has been observed, and the flow velocity increased mainly due to diamagnetic drift. The Pfirsch–Schlüter effect possibly explains the increase in the parallel flow velocity toward the plasma top at the outer mid-plane. The estimate by a simple expression of the Pfirsch–Schlüter flow supports this result. On the other hand, such a significant effect of drifts on parallel plasma flows cannot be seen in the inner and outer divertor regions.

The flow structure in the divertor region possibly affects the impurity transport and the in–out asymmetry. The detailed analysis for the impurity

transport and the in–out asymmetry will be discussed in the future.

References

[1] N. Tsois et al., J. Nucl. Mater. 266–269 (1999) 1230.
[2] N. Asakura et al., Nucl. Fusion 39 (1999) 1983.
[3] B.J. Braams et al., Fusion Technol. 9 (1986) 320.
[4] D. Reiter et al., Plasma Phys. Control. Fusion 33 (1991) 1579.
[5] R. Schneider et al., J. Nucl. Mater. 196–198 (1992) 810.
[6] A. Hatayama et al., Nucl. Fusion 40 (2000) 2009.
[7] A. Hatayama et al., in: Proceedings of the 19th IAEA Fusion Energy Conference, Lyon, France, October 2002.
[8] R. Schneider et al., Cont. Plasma Phys. 40 (2000) 328.
[9] V. Rozhansky et al., Cont. Plasma Phys. 40 (2000) 423.
[10] V. Rozhansky et al., Nucl. Fusion 41 (2001) 387.
[11] K. Hoshino et al., J. Nucl. Mater. 337–339 (2005) 276.
[12] K. Hoshino et al., Cont. Plasma Phys. 46 (2006) 116.
[13] N. Asakura et al., Plasma. Phys. Control. Fusion 44 (2002) 2102.
[14] N. Asakura et al., Nucl. Fusion 44 (2004) 503.
[15] D. Reiter et al., J. Nucl. Mater. 220–222 (1995) 987.
[16] P. Stangeby, The Plasma Boundary of Magnetic Fusion Devices, IOP, Bristol, 2000 (Chapter 18).